Imaging Science in Dentistry 2021; 51: 81-6
https://doi.org/10.5624/isd.20200253

Imaging features of Stafne bone defects on computed tomography: An assessment of 40 cases

Lucas Morita[1], Luciana Munhoz[1,*], Aline Yukari Nagai[1], Miki Hisatomi[2], Junichi Asaumi[2], Emiko Saito Arita[1]

[1]*Department of Stomatology, School of Dentistry, University of São Paulo, São Paulo, SP, Brazil*
[2]*Departament of Oral and Maxillofacial Radiology, Medical School, Okayama University, Okayama, Japan*

ABSTRACT

Purpose: This study was performed to assess and describe the imaging features of 40 cases of Stafne bone defects (SBDs) on computed tomographic (CT) examinations.

Materials and Methods: This study collected data, including age and sex, from 40 patients with SBDs who underwent CT exams. The imaging features of the SBDs were assessed in terms of their location, average size, the relationship of their contour with the cortical plate of the lingual mandible, bone margins, degree of internal density, shape, topographic relationship between the defect and the mandibular edge, the distance from the SBD to the base of the mandible, and the Ariji classification (type I, II, and III).

Results: The average age was 57.3 years (range, 28-78 years), and the patients were predominantly male (70%). In all cases (100%), the posterior unilateral lingual SBD variant was observed. Within the Ariji classification, type I was the most common (60%). Among the most frequently observed radiographic characteristics were thick sclerotic bone margin across the entire defect contour, completely hypointense internal content, an oval shape, and continuity with the mandibular base with discontinuity of the mandibular edge.

Conclusion: This study showed that posterior SBDs could present with an oval or rounded shape, complete hypodensity, and thick sclerotic margins. Likewise, SBDs could appear almost anywhere, with minor differences from the classic SBD appearance. It is fundamental for dental practitioners to know the imaging features of SBDs, since they are diagnosed primarily based on imaging. ***(Imaging Sci Dent 2021; 51: 81-6)***

KEY WORDS: Bone Cysts; Radiography, Panoramic; Salivary Glands; Multidetector computed tomography

Introduction

Stafne bone defects (SBDs) were first characterized as depressions in the mandible by Stafne in 1942.[1] SBDs are bone cavities that can be filled by salivary gland tissue, blood vessels, fatty tissue, or soft tissue.[2,3] A number of distinct names have been employed to designate SBDs, such as Stafne bone cysts, idiopathic bone cavities, developmental bone defects of the mandible, and ectopic salivary glands.[4,5]

Although the etiology of SBDs is uncertain, there are several theories regarding the origin of these cavities; for instance, it has been proposed that these depressions result from a hyperplastic glandular lobe, incomplete Meckel cartilage ossification, or abnormal vascular pressure from blood vessels.[5] The glandular hypothesis is the most widely accepted in the literature. According to this hypothesis, the cavity is formed in response to long-lasting pressure caused by a hyperplastic glandular lobe from submandibular, sublingual, or parotid glands in the lingual cortex of the mandible.[6-8]

SBD has a low prevalence of 0.13% in the general population[9-12] and is often located at the lingual margin of the posterior mandible, in the area that corresponds to the submandibular gland.[5] In rare cases, the depression is found in the mandible, in the area of the parotid gland[13] or the sublingual gland.[13,14] Moreover, there are 4 SBD variants: lingual posterior, lingual anterior, lingual ramus,

Received September 18, 2020; Revised October 26, 2020; Accepted November 13, 2020
*Correspondence to : Prof. Luciana Munhoz
Department of Stomatology, School of Dentistry, University of São Paulo, Av. Prof. Lineu Prestes, 2227, São Paulo, SP 05508-000, Brazil
Tel) 55-11-3091-7831, E-mail) dra.lucimunhoz@usp.br

Imaging Science in Dentistry · pISSN 2233-7822 eISSN 2233-7830

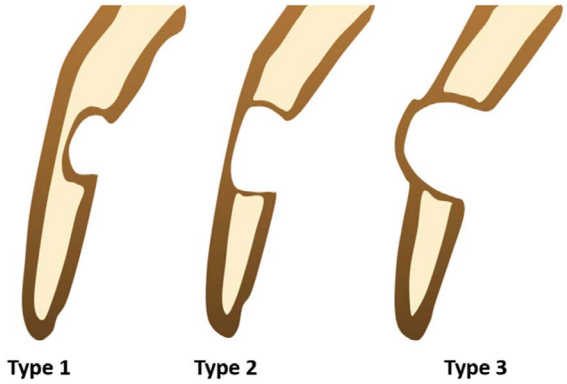

Fig. 1. Schematic illustration of Ariji et al. (1993).[17] Type 1: Defect bottom does not reach the buccal cortex. Type 2: Defect bottom reaches the buccal cortex without its expansion. Type 3: Buccal expansion of the cortical plate.

and buccal ramus.[5,6] On conventional radiographs (e.g., panoramic radiographs), SBD usually appears as oval or circular radiolucent area, with a radiopaque outline in the third molar region, below the roots.[5]

When further investigations are needed, computed tomography (CT) scans can also be performed in order to verify the depth and extension of the SBD, as well as to confirm its content.[5] CT is also useful to assess the anatomical relationships of SBDs with neighboring structures.[3,15,16]

The diagnosis of SBD is essentially based on imaging features. SBDs are often diagnosed in routine dental imaging examinations such as panoramic radiography. However, variations in the major imaging features of SBDs can occur, and a careful assessment is necessary to differentiate SBDs from other harmful intraosseous lesions.[5,13]

Hence, the objective of this research was to assess 40 SBD cases using multislice CT examinations, as well as to describe their average height and width (mean and range); relationship with the mandible lingual (buccal) cortical plate (based on the Ariji classification, which classifies the relationship of the bottom of the defect into types I, II, and III as illustrate in Figure 1);[17] bone margins (thin, thick, or without bone sclerosis); degree of internal density (hypodense or hyperdense); shape (rounded or oval); topographic relationship with the mandibular base; and distance to the mandibular base.

Materials and Methods

Forty SBD cases with available multidetector CT imaging examinations were selected. CT examinations with technical failures, lesions, or alterations in the area of interest were not included. Ethics committee approval was obtained from the university (number: CAAE 82037317.9.0000.0075). The guidelines of the Declaration of Helsinki were followed in this investigation.

The CT examinations were performed using an Aquilion One device (Toshiba Medical, Tokyo, Japan, 16 bits, 120 kVp, 300 mA) and the images were processed and measured using the same software (OsiriX MD viewer, ver. 11.0, Pixmeo, Switzerland, webpage: https://www.osirix-viewer.com/osirix/osirix-md/). The images were analyzed in all slices (axial, coronal, and sagittal), using an iMac desktop (8 GB, 2133 MHz, 27 inches).

First, data on the demographic characteristics of the patients with SBDs, such as age and sex, were collected, as well as the side affected by SBDs (left or right) on CT examinations. Next, the imaging features of the SBDs were analyzed by 4 observers (experts in oral and maxillofacial radiology), and the CT characteristics were described as follows: 1) average, maximum, and minimum size; 2) relationship of the outline with the mandibular lingual cortical plate according to the Ariji classification[17] (type I: the inferior limit of the cavity did not reach the buccal/lingual cortical plate, type II: the inferior limit of the cavity reached the cortical plate, but there was no expansion or distortion of the plate; and type III: the bottom of the concavity reached the buccal/lingual cortical plate and led to an expansion of the plate; Fig. 1); 3) bone margins (thin sclerosis, thick sclerosis, or no sclerosis; bone sclerosis was also classified as partial when sclerosis was not found along the entire contour of the defect or total when sclerosis was present on the entire contour of the defect); 4) internal density degree (partially hyperdense, completely hyperdense, or completely hypodense); 5) shape (oval or round); 6) the topographic relationship between the defect and the mandibular border (defect continuity to the inferior cortical line of the mandible [with or without visible discontinuity of the mandibular cortical cortex], defect contiguity with the mandibular base, and/or absence of contiguity/continuity with the mandibular border [the defect did not touch the mandibular base]); in the CT images, the aforementioned feature was assessed by evaluating the proximity of the SBD with the mandibular base; and 7) distance from the SBD to the inferior cortical line of the mandible (mean, maximum, minimum).

The average size, expressed as mean values, as well as the minimum and maximum values and the respective standard deviation, were calculated. The percentage of cases exhibiting the aforementioned imaging features was also presented. The statistical analysis (percentages

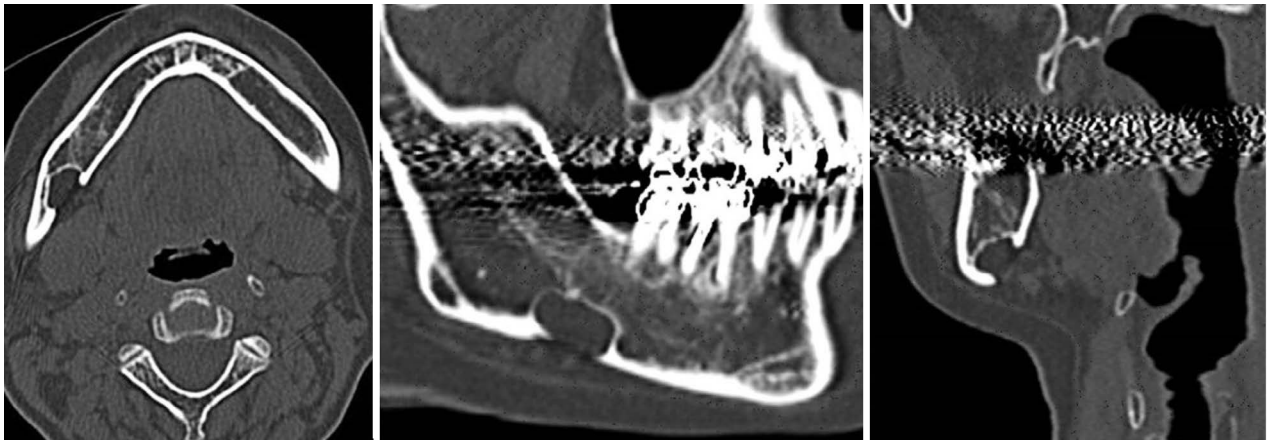

Fig. 2. Axial, sagittal, and coronal slices demonstrate hypodense internal content and the relationship of the defect with the inferior cortical line of mandible. The hypodense defect is continuous to the inferior cortical line of the mandible.

Fig. 3. Axial, sagittal, and coronal slices demonstrate the hypodense internal content and the relationship of the defect with inferior cortical line of mandible. In this case, the defect is below the third inferior molar and above the mandibular canal.

and average sizes) was performed using GraphPad Prism version 7.0 (GraphPad Prism Software, San Diego, CA, USA).

Results

Forty CT examinations containing SBDs were assessed. There were 28 (70%) male and 12 (30%) female patients. The mean age of the patients was 57.3 years (range, 28-78 years). In this investigation, the sample exclusively comprised the unilateral posterior variant. The left side (55%) was more frequently affected than the right side (45%). Figures 2 and 3 show 2 distinct cases in axial, sagittal, and coronal slices to illustrate this investigation. In Figure 2, the internal content of the defect is hypodense and the SBD shows continuity with inferior cortical line of the mandible. In Figure 3, it can be observed that the defect is above the mandibular canal, contiguous to the floor of the mandibular canal, and also continuous to the inferior cortical line of the mandible.

In terms of the classification proposed by Ariji et al.,[17] type I was the most frequently observed type (60% of cases). A thick sclerotic bone margin in the entire contour of the defect was the main radiographic feature found (70% of cases). All cases showed completely hypodense internal content. An oval shape was most commonly encountered (71.4%). Continuity with the inferior cortical line of the mandible was present in 46.1% of cases. The average height of the defect was 16.1 mm (in axial slices) and the average width was 17.5 mm (in coronal slices). The distance to the inferior cortical line of the mandible was 5.8 mm in axial slices and 5.2 mm in coronal slices. The radiographic features are presented in detail, along with the average sizes, in Tables 1 and 2.

Table 1. Imaging features of Stafne bone defects (SBDs) on multidetector computed tomographic images

Imaging Feature	Percentage (%)
Variant	
Posterior, unilateral	100 (40 cases)
Ariji classification[17]	
Type I	60.0
Type II	40.0
Type III	0.00
Bone margins	
Thin sclerosis	25.0
Partial	20.0
Total	5.0
Thick sclerosis	70.0
Partial	15.0
Total	55.0
Without sclerosis	5.0
Internal density degree	
Partially hypodense	0.0
Completely hypodense	100.0
Shape	
Rounded	28.5
Oval	71.4
Topographic relationship of SBD with the inferior cortical line of the mandible	
Continuity with the mandibular base	46.2
With discontinuity of the mandibular border	38.5
Without discontinuity of the mandibular border	7.7
Contiguity with the mandibular base	15.4
No contiguity with the mandibular base	38.5

Table 2. Measurements of Stafne bone defects on multidetector computed tomographic images

Average size (expressed as mean values)	Mean ± SD	Range
Height on axial image	16.1 ± 6.1	4.9-18.9
Width on coronal image	17.5 ± 5.3	4.7-21.0
Distance to mandibular base on axial image	5.8 ± 7.8	0.0-7.8
Distance to mandibular base on coronal image	5.2 ± 5.1	0.0-7.6

SD: standard deviation

Discussion

In the sample of the present study, SBDs were more frequently observed in men (70%) than in women (30%). Although the sample was relatively small, these findings align with those previously published in the literature.[6,10] Additionally, it has been reported that SBDs are often diagnosed in the fifth or sixth decade of life,[5,18] which is also in agreement with the present study, as the patients' mean age was 57.3 years.

Furthermore, the present sample comprised posterior SBDs, which is the most common presentation of mandibular SBDs. Although posterior SBDs are more frequent than other SBD types, the incidence of this defect is low, ranging from about 0.10% to 0.48% when diagnosed radiologically.[15]

Another presentation of SBDs is lingual anterior; this variation is less common, and usually appears in the region of premolars and canines. Lingual anterior SBDs are commonly mistaken for cystic lesions.[8,19,20] SBDs can also occur in the lingual ramus and buccal ramus, and these variations have been reported a few times in the literature.[13,21] In rare situations, SBDs can cause expansion of the buccal cortex.[22] Moreover, cases of intraorally exposed SBD, multiple SBDs, and double SBDs on the same side of the mandible have been reported in the literature.[23-25]

Posterior SBDs are easier to diagnose than other variants due to their exclusive location on radiographs.[4] CT examinations are requested only if there are doubts regarding the findings on panoramic radiographs or if the patient has any other complaint, such as pain or swelling in the affected area. In the cases included in the present study, multislice CT was requested in order to clarify other patient complaints, not exclusively to study the SBD itself.

The first imaging feature assessed in the present study was the classification published by Ariji et al.,[17] which considers the relationship of SBDs with the buccal cortical plate. The authors[17] stated that type I was the most prevalent, which agrees with the present findings. The mean measurements of height and width in this study are slightly higher than those obtained by Ariji et al.[17] Using panoramic radiographs, Hisatomi et al.[5] reported a mean height of 10.5 mm and a mean width of 14.3 mm; these differences are related to the type of imaging examinations and unique features of each sample.

In the analysis of the margins of the SBDs, thick sclerotic margins predominated, consistent with previous studies using panoramic radiographs.[5]

Although most SBDs are found in the posterior region of the mandible, Aps et al. recently showed that SBDs appeared almost everywhere in the mandible, and their interior was filled with soft tissue.[26] In cases of SBDs with unusual imaging features, sialography also can be per-

formed in order to exclude other lesions, especially if the defect contains glandular tissue, since the ductular system can be detected using sialography.[27]

Magnetic resonance imaging (MRI) allows the detailed differentiation of soft tissues, and has the advantage of not exposing the patient to ionizing radiation.[28,29] The disadvantages of MRI are its high cost, the inability to perform the examination in claustrophobic patients, and the generation of image artifacts if the patient has orthodontic devices or protheses that cannot be removed during the examination.

Currently, CT examinations are more accessible than other imaging modalities both in medicine and in dentistry, and are more often requested in a wide range of situations. Since SBDs can appear as a concomitant imaging finding, clinicians should be familiar with the main imaging features of SBDs in order to avoid misdiagnosis.

In conclusion, posterior variants of SBDs frequently present as oval or rounded cavities, with hypodense internal content and thick sclerotic margins on CT examinations. Knowledge of the imaging features of SBDs in each imaging modality, along with clinical experience, is essential to diagnose this condition correctly.

Conflicts of Interest: None

References

1. Stafne EC. Bone cavities situated near the angle of the mandible. J Am Dent Assoc 1942; 29: 1969-72.
2. Kaya M, Ugur KS, Dagli E, Kurtaran H, Gunduz M. Stafne bone cavity containing ectopic parotid gland. Braz J Otorhinolaryngol 2018; 84: 669-72.
3. Minowa K, Inoue N, Sawamura T, Matsuda A, Totsuka Y, Nakamura M. Evaluation of static bone cavities with CT and MRI. Dentomaxillofac Radiol 2003; 32: 2-7.
4. Taysi M, Ozden C, Cankaya B, Olgac V, Yildirim S. Stafne bone defect in the anterior mandible. Dentomaxillofac Radiol 2014; 43: 20140075.
5. Hisatomi M, Munhoz L, Asaumi J, Arita ES. Stafne bone defects radiographic features in panoramic radiographs: assessment of 91 cases. Med Oral Patol Oral Cir Bucal 2019; 24: e12-9.
6. Philipsen HP, Takata T, Reichart PA, Sato S, Suei Y. Lingual and buccal mandibular bone depressions: a review based on 583 cases from a world-wide literature survey, including 69 new cases from Japan. Dentomaxillofac Radiol 2002; 31: 281-90.
7. Choukas NC, Toto PD. Etiology of static bone defects of the mandible. J Oral Surg Anesth Hosp Dent Serv 1960; 18: 16-20.
8. de Courten A, Küffer R, Samson J, Lombardi T. Anterior lingual mandibular salivary gland defect (Stafne defect) presenting as a residual cyst. Oral Surg Oral Med Oral Pathol Oral Radiol Endod 2002; 94: 460-4.
9. Assaf AT, Solaty M, Zrnc TA, Fuhrmann AW, Scheuer H, Heiland M, et al. Prevalence of Stafne's bone cavity - retrospective analysis of 14,005 panoramic views. In Vivo 2014; 28: 1159-64.
10. Sisman Y, Miloglu O, Sekerci AE, Yilmaz AB, Demirtas O, Tokmak TT. Radiographic evaluation on prevalence of Stafne bone defect: a study from two centres in Turkey. Dentomaxillofac Radiol 2012; 41: 152-8.
11. Chen CY, Ohba T. An analysis of radiological findings of Stafne's idiopathic bone cavity. Dentomaxillofac Radiol 1981; 10: 18-23.
12. Oikarinen VJ, Julku M. An orthopantomographic study of developmental mandibular bone defects (Stafne's idiopathic bone cavities). Int J Oral Surg 1974; 3: 71-6.
13. Hisatomi M, Munhoz L, Asaumi J, Arita ES. Parotid mandibular bone defect: a case report emphasizing imaging features in plain radiographs and magnetic resonance imaging. Imaging Sci Dent 2017; 47: 269-73.
14. Ozaki H, Ishikawa S, Kitabatake K, Yusa K, Tachibana H, Iino M. A case of simultaneous unilateral anterior and posterior Stafne bone defects. Case Rep Dent 2015; 2015: 983956.
15. Quesada-Gómez C, Valmaseda-Castellón E, Berini-Aytés L, Gay-Escoda C. Stafne bone cavity: a retrospective study of 11 cases. Med Oral Patol Oral Cir Bucal 2006; 11: E277-80.
16. Schneider T, Filo K, Locher MC, Gander T, Metzler P, Grätz KW, et al. Stafne bone cavities: systematic algorithm for diagnosis derived from retrospective data over a 5-year period. Br J Oral Maxillofac Surg 2014; 52: 369-74.
17. Ariji E, Fujiwara N, Tabata O, Nakayama E, Kanda S, Shiratsuchi Y, et al. Stafne's bone cavity. Classification based on outline and content determined by computed tomography. Oral Surg Oral Med Oral Pathol 1993; 76: 375-80.
18. He J, Wang J, Hu Y, Liu W. Diagnosis and management of Stafne bone cavity with emphasis on unusual contents and location. J Dent Sci 2019; 14: 435-9.
19. Smith MH, Brooks SL, Eldevik OP, Helman JI. Anterior mandibular lingual salivary gland defect: a report of a case diagnosed with cone-beam computed tomography and magnetic resonance imaging. Oral Surg Oral Med Oral Pathol Oral Radiol Endod 2007; 103: e71-8.
20. Sisman Y, Etöz OA, Mavili E, Sahman H, Tarim Ertas E. Anterior Stafne bone defect mimicking a residual cyst: a case report. Dentomaxillofac Radiol 2010; 39: 124-6.
21. Lee KC, Yoon AJ, Philipone EM, Peters SM. Stafne bone defect involving the ascending ramus. J Craniofac Surg 2019; 30: e301-3.
22. Flores Campos PS, Oliveira JA, Dantas JA, de Melo DP, Pena N, Santos LA, et al. Stafne's defect with buccal cortical expansion: a case report. Int J Dent 2010; 2010: 515931.
23. Nishimura S, Osawa K, Tanaka T, Imamura Y, Kokuryo S, Habu M, et al. Multiple mandibular static bone depressions attached to the three major salivary glands. Oral Radiol 2018; 34: 277-80.
24. Ozdede M. An unusual case of double stafne bone cavities. Surg Radiol Anat 2020; 42: 543-6.
25. Dereci Ö, Duran S. Intraorally exposed anterior Stafne bone

defect: a case report. Oral Surg Oral Med Oral Pathol Oral Radiol 2012; 113: e1-3.
26. Aps JK, Koelmeyer N, Yaqub C. Stafne's bone cyst revisited and renamed: the benign mandibular concavity. Dentomaxillofac Radiol 2020; 49: 20190475.
27. Li B, Long X, Cheng Y, Wang S. Cone beam CT sialography of Stafne bone cavity. Dentomaxillofac Radiol 2011; 40: 519-23.
28. Segev Y, Puterman M, Bodner L. Stafne bone cavity - magnetic resonance imaging. Med Oral Patol Oral Cir Bucal 2006; 11: E345-7.
29. Probst FA, Probst M, Maistreli IZ, Otto S, Troeltzsch M. Imaging characteristics of a Stafne bone cavity - panoramic radiography, computed tomography and magnetic resonance imaging. Oral Maxillofac Surg 2014; 18: 351-3.